PVP-Vol. 343, Development, Validation, and Application
of Inelastic Methods for Structural Analysis and Design
ASME 1996

REVIEW OF BUCKLING MODE AND GEOMETRY EFFECTS ON POSTBUCKLING STRENGTH OF CORRUGATED CONTAINERS

Thomas J. Urbanik

U.S. Department of Agriculture, Forest Service
Forest Products Laboratory[1]
One Gifford Pinchot Drive
Madison, Wisconsin 53705-2398
608-231-9428 Fax (608)231-9592

ABSTRACT

Various postbuckling models involving elastic versus inelastic buckling, linear versus nonlinear material characterization, and finite versus infinite length plate geometry were fit to historical data on compression strength of corrugated fiberboard box and tube specimens. The objectives were to determine if the buckling mode shape could be predicted and if inelastic buckling failure could be differentiated from elastic failure in the side panel and end panel components to account for specimen geometry and material property effects. The variation of a normalized panel strength with a panel slenderness was the criterion for discerning among alternative models. In some cases multiple solutions were feasible. Overall, a finite length plate theory, combined elastic-inelastic postbuckling model, and nonlinear material characterization with plate stiffness empirically corrected with respect to its aspect ratio consistently fit each data source.

NOMENCLATURE

A_0	Buckling perturbation amplitude
c_1, c_2	Stress-strain constants
$\hat{c}$	Normalized in-plane shear modulus of elasticity (Urbanik, 1992)
d, l, h	Plate length, width, and thickness
D_x, D_y	Plate bending stiffness per unit width perpendicular and parallel to plate axis
$\overline{EI}_x, \overline{EI}_y$	Fiberboard bending stiffness per unit width perpendicular and parallel to fluting axis
f	Normalized buckling strain function, Eq. (14)
K	Buckling coefflcient, Eq. (3)
m, m_i	Number of buckled half-waves along d and integer component of m
P	Box compression strength
p, λ, χ, χ_i	Buckled wave period, wave frequency, and normalized wave frequencies
P_{cr}, P_f, P_y	Plate critical load, applied failure load, and material yield load per unit width
S	Normalized plate stiffness, Eq. (7)
U	Universal plate slenderness $\sqrt{P_y/P_{cr}}$
x, y	Plate Cartesian coordinates perpendicular and parallel to plate axis
W	Buckling perturbation function, Eq. (5)
α, η	Postbuckling constants
β	Characteristic equation root
$\varepsilon, \sigma, \sigma_u$	Strain, stress, and ultimate stress
$\hat{\varepsilon}, \hat{\varepsilon}_i, \hat{\sigma}$	Normalized buckling strains and buckling stress
ν, ν_1, ν_2	Geometric mean $\sqrt{\nu_1 \nu_2}$ of Poisson's ratio associated with x- and y-direction plate loading
ϕ	Effective plate aspect ratio, Eq. (4)
τ	Empirical stiffness correction
θ_0	Nonlinear material postbuckling constant c_1/σ_u

[1]The Forest Products Laboratory is maintained in cooperation with the University of Wisconsin. This article was written and prepared by U. S. Government employees on offrcial time, and it is therefore in the public domain and not subject to copyright.

INTRODUCTION

The corrugated fiberboard box is the most common containment unit employed somewhere along the distribution and storage cycle of almost every packaged product. For stacking applications, box top-to-bottom compression strength is the most common performance characteristic. The traditional box compression formula by McKee et al. (1963)[2] is essentially a restructuring of terms in an empirical postbuckling formula (Bulson, 1969) applicable to thin plates made from a linear material. The McKee formula is limited to regular slotted-style containers, the most general in use, when the length does not exceed three times the width and the perimeter does not exceed seven times the depth.[3]

For commercial utility, McKee et al. (1963) advocated treating a rectangular box as a square box of equal perimeter and modeling each supporting panel as an infinitely long, simply supported plate. Material yield strength, panel bending stiffness along the two principal axes, and panel width are the inputs to the formula. Within the limits of their data base, the McKee formula was accurate to within 6.1% on average.

Recent issues in box design have raised concerns about the relevance of the McKee formula for boxes other than regular slotted containers and for shallow boxes. Statistical formulas (Maltenfort, 1957) have demonstrated a greater sensitivity to box length and width effects than predictable by the McKee formula. Elastic boundary conditions examined in work by Bulson (1969) introduce a more significant length sensitivity of buckled plates than that allowed by the McKee formula. Finite element techniques (Pommier et al., 1991) have been used to elucidate the effect of additional elastic constants, besides bending stiffness, of corrugated fiberboard on box compression strength.

The incorporation of nonlinear material theory from work by Urbanik and others (Johnson and Urbanik, 1987; Urbanik, 1992) into the postbuckling formula (Bulson, 1969) made the box compression model of Urbanik (in preparation) more sensitive to length and width differences. Linear material theory was shown to overpredict the strength of narrow box panels, typically the end panels, and to lead to an apparent strength equality between rectangular and square boxes of the same perimeter. Nonlinear material theory was shown to predict a lower buckling strength for low width panels and be consistent with the Maltenfort (1957) data. The research by Urbanik (in preparation) was limited to a single data base (McKee et al., 1963); box depth was not considered, and failure by elastic buckling was assumed. This report generalizes the theory (Urbanik, in preparation) further and examines additional unpublished industry data (Batelka and Smith, 1993; Hutten and Brodeur, 1995; IPC, 1967). The objective was to determine if the buckling mode shape can be predicted and if inelastic buckling failure of panel components can be differentiated from elastic failure to account for box depth and material property effects.

[2] Hereafter referred to as the McKee formula

[3] Box length, width, and depth refer to dimensions of the unfolded blank regardless of box orientation. Plate or panel length and width refer to the principle axes coinciding with the loading and transverse directions, respectively.

BUCKLING THEORY

Linear Material

Infinite Length Plate. The critical load P_{cr} of a simply supported, infinitely long plate subjected to longitudinal in-plane compression is obtainable from Bulson (1967) and was presented by Urbanik (in preparation) in the form

$$P_{cr} = \frac{4\pi^2\sqrt{D_x D_y}}{l^2} \tag{1}$$

Box compression strength P is the sum $\sum P_f$ of failure loads predicted by applying the empirical formula (Bulson, 1967)

$$\frac{P_f}{P_y} = \alpha\left(\frac{P_{cr}}{P_y}\right)^{\eta} \tag{2}$$

to the end and side panel components. Material yield strength P_y is the edgewise compression strength of the corrugated fiberboard.

Finite Length Plate. A more general prediction of P_{cr} for plates having a finite length d is obtained by multiplying the critical load from Equation (1) by the buckling coefficient

$$K = \frac{1}{4}\left(\frac{m^2}{\phi^2} + \frac{\phi^2}{m^2}\right) + \frac{1}{2} \tag{3}$$

where m is the number of buckled half-waves along d and ϕ is an effective plate aspect ratio given by

$$\phi = \frac{d}{l}\left(\frac{D_x}{D_y}\right)^{1/4} \tag{4}$$

The variation of K with ϕ shown in Figure 1 can be compared with figure 2.3 in Bulson (1969).

Nonlinear Material

Infinite Length Plate. The nonlinear material behavior introduced by Johnson and Urbanik (1987) is applicable to infinitely long plates made from paper characterized by the stress-strain relation $\sigma = c_1 \tanh(c_2\varepsilon / c_1)$. A solution to the differential equation of buckling was derived by considering buckling modes of the form

$$W = A_0 e^{i\lambda y + \beta x} \tag{5}$$

and superimposing them to obtain a fourth-order characteristic equation for $\beta(\lambda)$. In Equation (5), λ is a wave frequency in the y-direction, the plate axis, and has units of radians per unit length. A normalized wave frequency χ was given by equation 2.10 of Johnson and Urbanik as

$$\chi = \frac{l\lambda}{2}\left(\frac{\nu_2}{\nu_1}\right)^{1/4} = \frac{l\lambda}{2}\left(\frac{D_y}{D_x}\right)^{1/4} \tag{6}$$

and the solution for a normalized buckling strain $\hat{\varepsilon}$ as a function of χ was determined. The optimum χ that yields a minimum $\hat{\varepsilon}$ corresponds to buckling of an infinitely long plate. The algorithm (Johnson and Urbanik, 1987) for obtaining $\hat{\varepsilon}(\chi)$ (χ) of an infinitely long plate is summarized in the Appendix. The normalized buckling stress $\hat{\sigma}$ from equation 5.1 of Johnson and Urbanik is $\hat{\sigma} = \tanh \tanh \hat{\varepsilon}$.

The variation of $\hat{\sigma}$ as a function of a normalized plate stiffness

$$S = \frac{c_2}{c_1}\left(\frac{h}{l}\right)^2\sqrt{\frac{\nu_1}{\nu_2}} = \frac{12\sqrt{\overline{EI}_x\overline{EI}_y}}{\theta_0 P_y l^2} \tag{7}$$

was examined by Johnson and Urbanik [1987). The first form of S in Equation (7) is useful when all the respective material constants can be obtained. The second form of S was derived by Urbanik (in preparation) for corrugated fiberboard for which edgewise compression strength and bending stiffness are normally obtainable. The constant $\theta_0 = c\ 1/\sigma_u$ induces an average curvature to the stress–strain relation, and as θ_0 approaches ∞, the nonlinear buckling theory approaches the linear theory. The second form of S predicts the ratio $P_{cr}/P_y = \theta_0\hat{\sigma}$ (Urbanik, in preparation) and enables Equation (2) to be applied to the postbuckling response of a nonlinear material.

Finite Length Plate. Equation (5) is applicable to finite length plates if λ is chosen to yield W = 0 at the plate boundaries. For this case, the buckling strain will be slightly greater than the optimum $\hat{\varepsilon}$ as restricted by an integral number of buckled half-waves along the plate axis. The period of the buckled wave is $p = 2\pi/1$. from which the number m of half-waves along d is given by

$$m = \frac{2d}{p} = \frac{2\chi\phi}{\pi} \tag{8}$$

The levels of buckling strain corresponding to the integer component $m\ 1$ of m and to $m_2 = m_1 + 1$ need to be examined.

The theory of Johnson and Urbanik (1987) is further generalized in the Appendix for determining the buckling response of a plate having a finite length. The analysis starts with a determination of the optimum χ for the infinitely long plate. Values of χ_1 and χ_2 that are close to the optimum value and yield integer numbers m_1 and m_2, respectively, of half-waves are given by

$$\chi_i = \frac{m_i\pi}{2\phi} \qquad i = 1,2 \tag{9}$$

The analysis continues with a determination of $\hat{\varepsilon}_1$ and $\hat{\varepsilon}_2$ corresponding to fixed χ_1 and χ_2, respectively. The buckling strain of the finite length plate is then the lower of&l and $\hat{\varepsilon}_2$.

The variation of $\hat{\sigma}$ with S is shown in figure 2 of Johnson and Urbanik (1987) for the case of infinitely long plates. Figure 2 herein shows how the $\hat{\sigma}$ ratio between finite and infinite length plates varies with ϕ at various levels of S. As S approaches 0, the $\hat{\sigma}$ ratio approaches K. As ϕ approaches infinity, the variation of the $\hat{\sigma}$ ratio with S shown in Figure 2 at discrete levels is the same as the variation of $\hat{\sigma}$ with S shown in figure 2 of Johnson and Urbanik (1987) over a continuous range.

Short/Long Plate Criterion. Figures 1 and 2 predict that when plate buckling occurs with two or more half-waves, buckling strength is relatively insensitive to plate length. However. if plates are short enough to constrain buckling to a single half-wave, buckling strength becomes increasingly sensitive to plate length as ϕ decreases. As shown in Figure 2, as S increases (i.e., for increasingly nonlinear materials), approximating a plate with an infinite length becomes accurate for shorter plates.

A criterion for differentiating between short and long plates can be had by considering the buckling theory when $m = 1$. When $m = 1$, Equation (8) predicts that $\chi = \pi/2\phi$. Making this substitution into equation 3.2' of Urbanik (1992) gives an expression for buckling strain in terms of ϕ when buckling occurs with one half-wave:

$$\hat{\varepsilon} = \frac{\pi^2 S}{12\phi^2}\left[\frac{1}{1-\nu^2}(\hat{c}+\phi)^2 - \frac{\hat{c}^2-1}{1-\nu^2} - f(\hat{\varepsilon})\right] \tag{10}$$

Differentiating this expression with respect to ϕ and equating the result to 0 yields the value of ϕ, below which plates become increasingly sensitive to plate length.

$$\phi = \left[\frac{\nu^2 e^{4\hat{\varepsilon}} + 4\hat{\varepsilon}e^{2\hat{\varepsilon}}(1-\nu^2) - \nu^2}{e^{4\hat{\varepsilon}} - 1}\right]^{1/4} \tag{11}$$

Equation (11) is plotted in Figure 3.

RESULTS

Box compression strength data were obtained from previously reported tests on complete corrugated boxes, including the top and bottom flaps (McKee et al., 1963; IPC, 1967) and corrugated tubes, i.e., boxes without flaps (Batelka and Smith, 1963; Hutten and Brodeur, 1995). A tube specimen would be expected to yield a more rigid boundary condition along the horizontal loading edge, compared to a box specimen. A more complete description of the data can be had from the referenced sources. In this study, data are normalized with respect to ϕ and a universal slenderness $U = \sqrt{P_y/P_{cr}}$.

Elastic Buckling

Elastic buckling is characterized by applying Equation (2), assuming that all box panels fail by elastic buckling. The curve-fitting procedure is discussed in detail in another report (Urbanik, in preparation). As mentioned previously, when material is characterized as nonlinear the expression $\theta_0\hat{\sigma}$ is substituted for P_{cr}/P_y in Equation (2).

Table I-Characterization of elastic postbuckling response–Infinite length

Data source[a]	Material character-ization	Postbuckling constant α	η	θ_0	Avg. error mag-nitude (%)
McKee et al. 1963	Linear	0.397	-0.255	∞	6.08
	Nonlinear	0.434	-0.308	1.13	5.83
IPC 1967 (S)	Linear	0.289	-0.048	∞	7.25
	Nonlinear	0.289	-0.048	∞	7.25
IPC 1967 (L)	Linear	0.540	-0.461	∞	6.03
	Nonlinear	0.540	-0.461	∞	6.03
Batelka & Smith 1993	Linear	0.681	-0.233	∞	11.2
	Nonlinear	0.717	-0.276	2.41	11.0
Hutten & Brodeur 1995	Linear	0.479	-0.021	∞	9.35
	Nonlinear	0.479	.021	∞	9.35

[a]S refers to small boxes; L to large boxes.

Table II-Characterization of elastic postbuckling response–Finite length

Data source	Material character-ization	Postbuckling constant α	η	θ_0	Avg error mag-nitude (%)
McKee et al. 1963	Linear	0.384	-0.247	∞	6.42
	Nonlinear	0.428	-0.319	1.12	6.02
IPC 1967 (S)	Linear	0.290	-0.055	∞	7.26
	Nonlinear	0.290	-0.055	∞	7.26
IPC 1967 (L)	Linear	0.528	-0.459	∞	6.05
	Nonlinear	0.528	-0.459	∞	6.05
Batelka & Smith 1993	Linear	0.638	-0.279	∞	8.78
	Nonlinear	0.928	-0.617	0.87	5.72
Hutten & Brodeur 1995	Linear	0.532	-0.381	∞	5.98
	Nonlinear	0.532	-0.381	∞	5.98

Infinite Length Model. In another study (Urbanik, in preparation), the four postbuckling models involving the combinations of square versus rectangular box geometry and linear versus nonlinear material characterization were tested against the data from McKee et al. (1963). In the work reported here, comparisons among the rectangular geometry of linear and nonlinear postbuckling models were extended for additional data sources (Table I). The Institute of Paper Chemistry (IPC) data in Table I are divided into small-box (S) and large-box (L) subsets because the optimum θ_0 found to fit the combined data was less that 0.1, an infeasible solution. Nonlinear material characterization of the IPC data and Hutten and Brodeur (1995) data yielded $\theta_0 = \infty$ and reflects the insensitivity of the elastic postbuckling-infinite length model to nonlinear material effects within these data.

In the preceding analysis, it was assumed that box panels had an infinite length and that the wave period of buckling in the side panel was independent of the wave period in the end panel. An assessment of this assumption was made by plotting Equation (3), based on a linear material characterization, through the data **of** each data source (Figs. 4–7). The high accuracy of the infinite length model applied to the McKee et al. and IPC data (Table I) can be attributed to the low sensitivity of P_{cr} to d predicted by Figures 4 and 5, wherein $K < 2$ for all the data. By contrast, the data from the other studies (Table 1) yielded less accuracy and greater K levels (Figs. 6, 7). The lower accuracy of a simply supported plate model applied to these data might also have resulted from a stiffer boundary condition along the loaded edges of the tube specimens.

Finite Length Model. The finite length plate model was next applied to the data and various rules were examined for characterizing the buckling mode shape. Criteria for selecting the value of m were as follows:

1. The value of m that yielded the weakest P_{cr} for each panel, so that side and end panels could buckle into different numbers of half-waves. This criterion is consistent with a simply supported edge condition in which no bending moment gets transferred and no interaction occurs across the vertical score-line.
2. The value of m that yielded the weakest P, so that side and end panels would buckle into the same number of half-waves. This criterion is consistent with a rigid connection between the panels.
3. The value of m that yielded the lowest P_{cr} for the side panel, which was applied to side and end panels.
4. The value of m that yielded the lowest P_{cr} for the end panel, which was applied to side and end panels.

Criteria 3 and 4 are strictly empirical. Results based on criterion 3 are given in Table II. As expected from the number of specimens sensitive to box depth (Figs. 5, 6), the finite length model produced better results for the data from Batelka and Smith (1993) and Hutten and Brodeur (1995). However, aecuraey decreased for the McKee et al. and IPC data. Additional tests and analysis are needed to determine the reason.

Elastic-Inelastic Buckling

Figure 8 shows a fit of Equation (2) to the Batelka and Smith (1993) data, following the technique presented in Urbanik (in preparation). Axes are scaled to show the variation of a normalized strength P/P_y with U. From the clustering of data around $U = 1.07 = 1\sqrt{0.87}$, it can be inferred that a different failure mechanism occurred in the box panels represented by these points. A more general postbuckling formula characterizing the combination of elastic and inelastic buckling modes of failure is given by

Table III-Characterization of elastic-inelastic postbuckling response–Finite length

Data source	Material character-ization	Postbuckling constant α	η	θ_0	Avg error mag-nitude (%)
McKee et al. 1963	Linear	0.405	-0.289	∞	6.18
	Nonlinear	0.436	-0.329	1.00	6.04
IPC 1967 (S)	Linear	0.290	-0.055	∞	7.26
	Nonlinear	0.290	-0.055	∞	7.26
IPC 1967 (L)	Linear	0.528	-0.459	∞	6.05
	Nonlinear	0.528	-0.459	∞	6.05
Batelka & Smith 1993	Linear	0.773	-0.505	∞	5.11
	Nonlinear	0.773	-0.505	∞	5.11
Hutten & Brodeur 1995	Linear	0.523	-0.349	∞	6.00
	Nonlinear	0.550	-0.444	3.30	5.77

$$\frac{P_f}{P_y} = \alpha\left(\frac{P_{cr}}{P_y}\right)^{\eta} \quad U > 1$$
$$\frac{P_f}{P_y} = 1 \quad U \le 1 \tag{12}$$

The results of fitting the elastic-inelastic buckling model to the previous data are given in TableIII. A tit of Equation (12) to the Batelka and Smith data (Fig. 9) yields a seemingly more rational distribution of points compared to Figure 8.

STIFFNESS CORRECTION

Expression of Correction

Theory (March and Smith, 1945) predicts that the magnitude of K in Equation (3) varies with the distribution of the shearing modulus of elasticity through the thickness of the plate. In figure 2.13 in Bulson (1969), the relative minima displayed by the cusps in Figure 1 are predicted to increase from right to left as the loaded edges are made more rigid. Neither the nonhomogeneous nature of corrugated fiberboard nor the elasticity of the boundary condition along loaded edges was made art input to the prediction of P_{cr} by Equation (1).

A successful criterion found to empirically correct for stiffening effects attributable to variations in shearing modulus of elasticity and boundary condition elasticity was to modify the expression for S and characterize panel stiffness with the apparent stiffness given by

$$S = \phi^{\tau}\frac{12\sqrt{\overline{EI}_x\overline{EI}_y}}{\theta_0 P_y l^2} \tag{13}$$

where τ is an empirical stiffness correction.

Table IV–Characterization of elastic–inelastic postbuckling response–Finite length and corrected *S*

Data source	S-correction τ	Postbuckling constant α	η	θ_0	Avg. error mag-nitude (%)
McKee et al. 1963	0.184	0.429	-0.320	1.02	5.99
IPC 1967	0.760	0.413	-0.332	∞	7.14
Batelka & Smith 1993	-0.371	0.798	-0.563	1.24	3.79
Hutten & Brodeur 1995	-0.323	0.558	-0.455	1.90	4.35

Results of Correction

Results of applying Equation (13) as art input to the postbuckling model by Equation (12) and using mode criterion 3 are given in Table IV. The IPC S-subset and L-subset were combined, and the prediction errors for all the data sources were found to be independent of specimen depth. Equation (12) is plotted through each data source in Figures 10–13.

DISCUSSION

The results shown in Table IV are consistent with the stress–strain behavior of paper and with the effect of elastic loading edges on plate buckling strength. With the exception of the IPC data, the average $\theta_0 = 1.39$ predicted for corrugated fiberboard compares very well with $\theta_0 = 1.33$ determined experimentally for paper (Urbanik, 1990). An infinite θ_0 value for the IPC data resulted from the insensitivity of high slenderness panels (Fig. 11) to nonlinear material effects and a numerical condition for which arbitrarily large values of θ_0 yield equally good results. Low slenderness panels failing by inelastic buckling (Figs. 10, 12, 13) provide a more severe test of nonlinear material effects.

McKee et al. (1963) did not observe a depth sensitivity of box compression specimens, and this is reflected in the low value of τ (Table IV). A value of $\tau > 0$ for the IPC data predicts that box strength increases with depth and is contrary to theory. Because the IPC data consisted of only two box sizes (thus explaining the compact ϕ data in Fig. 5), a value of $\tau > 0$ may have resulted from fabrication differences between the two sizes. A value of $\tau < 0$ for the other data in Table IV (Batelka and Smith, 1993; Hutten and Brodeur, 1995) leads to an apparent stiffening of panel components as box depth and the corresponding number of buckled half-waves decrease, and this value is consistent with the buckling of plates with loaded edges fixed and unloaded edges simply supported (Bulson, 1969). These tests were on tube specimens and the obtained values of τ yield a measure of the boundary condition elasticity along the loaded edges. The horizontal score between the box flaps and box panels of specimens from the McKee et al. and IPC studies indicates a performance closer to a simply supported condition.

The analysis results in Tables II–IV are based on mode criterion 3 applied to each data source. The effects of the assumed mode shape on the finite length models were quantified by fitting models based on the various combinations of linear versus nonlinear, elastic versus elastic–inelastic, and mode criteria 1–4 to each data source. When mode criterion 2 was used, the minimum sum of errors squared obtained from each model was on average 22% greater than the average minima obtained from mode criterion 3. Mode criterion 4 yielded a 56% greater average than that obtained from criterion 3. Mode criteria 2 and 4 were thus rejected. Mode criterion 1, when applied to the nonlinear, elastic-inelastic model tit to the Batelka and Smith (1993) data, yielded a minimum sum of errors squared that was 3% less than the minimum obtained from mode criterion 3. So, these data offer some evidence that mode criterion 1 is a better choice. However. mode criterion 3 enabled all of the IPC data to be unified in the corrected stiffness model, and it was thus selected and applied consistently to all the data.

CONCLUSION

In a review of various postbuckling models fit to historical data on box compression strength, a model developed from finite length plate theory, combined elastic-inelastic failure mechanism, and nonlinear material characterization with plate stiffness empirically corrected with respect to its aspect ratio consistently fit each data source. Simplified models based on infinite length plates, elastic failure, or linear material fit box strength data more accurately than they fit tube strength data when the ranges of panel aspect ratio and universal slenderness were broad. The shape predicted by the wider box panel under simply supported conditions, and applied to the narrower panel, was the best predictor of the box buckling mode. The shape predicted by independent buckling of panels was more accurate for tube specimens. Stiffening effects attributable to edge condition elasticity and shearing stiffness, but not experimentally determinable, could be empirically accounted for by correcting the normalized panel stiffness. The corrected model predicts an average shape of the nonlinear stress-strain curve of corrugated fiberboard from compression strength and bending stiffness data. A plot of normalized strength varying with universal slenderness is useful to differentiate between elastic and inelastic failure modes and to verify the significance of nonlinear material effects.

ACKNOWLEDGMENT

Appreciation is extended to the Containerboard and Kraft Paper Group of the American Forest & Paper Association for permission to use the unpublished sources of industry data.

REFERENCES

Batelka, J.J., and Smith, C.N., 1993, "Package Compression Model," Containerboard and Kraft Paper Group of the American Forest & Paper Association, Project 3746, Final Report, February.

Bulson, P.S., 1969, "The Stability of Flat Plates," American Elsevier Publishing Company, Inc., NY.

Hutten, M., and Brodeur, P., 1995, "MD and CD Properties of Linerboard Components and the Resulting Box Stacking Performance," Containerboard and Kraft Paper Group of the American Forest & Paper Association, Project 3912, Final Report, July.

IPC, 1967, "The Effect of Distribution of Stiffness Between Components on the Compressive Performance of Corrugated Boxes," Testing, Compression 85, Project 2695-3, Institute of Paper Chemistry, pp. 1–52.

Johnson, M.W., Jr., and Urbanik, T.J., 1987, "Buckling of Axially Loaded, Long Rectangular Paperboard Plates," Wood and Fiber Science, Vol. 19(2), pp. 135–146.

Maltenfort, G.G., 1956, "Compression Strength of Corrugated Containers," Fibre Containers, Vol. 41(7), July.

March, H. W., and Smith, C.B., 1945, "Buckling Loads of Flat Sandwich Panels in Compression. Various Types of Edge Conditions," Report 1525, U. S. Department of Agriculture, Forest Service, Forest Products Laboratory, Madison, WI.

McKee, R.C., Gander, J.W., and Wachuta, J.R., 1963, "Compression Strength Formula for Corrugated Boxes," Paperboard Packaging, August.

Pommier, J.C., Poustis, J., Fourcade, E., and Morlier, P., 1991, "Determination of the Critical Load of a Corrugated Cardboard Box Submitted to Vertical Compression by Finite Elements Methods," Proceedings, International Paper Physics Conference, TAPPI, Atlanta, GA, pp. 437–447.

Urbanik, T.J., 1990, "Correcting for Instrumentation With Corrugated Fiberboard Edgewise Crush Test Theory," Tappi Journal, October pp. 263–268.

Urbanik, T.J., 1992, "Effect of In-Plane Shear Modulus of Elasticity on Buckling Strength of Paperboard Plates," Wood and Fiber Science, Vol. 24(4), pp. 381–384.

Urbanik, T.J., "Linear and Nonlinear Material Effects on Postbuckling Strength of Corrugated Containers." Submitted to Tappi Journal.

APPENDIX

Algorithms for determining the buckling stress of a simply supported plate with compression in the direction of its length and having a nonlinear material characterization are as follows:

1. Input S, ϕ, v, and $\hat{c}$. If the Poisson's ratio cannot be determined, let $v = 0$. If the in-plane shear modulus of elasticity cannot be determined, let $\hat{c} = 1$.

2. Define function $f(\hat{\varepsilon})$ from Johnson and Urbanik (1987).

$$f(\hat{\varepsilon}) = 1 - \frac{2\hat{\varepsilon}}{\sinh(2\hat{\varepsilon})} \tag{14}$$

Infinite Length-Optimum χ

3. Determine an initial $\hat{\varepsilon}$ from equation 3.5' of Urbanik (1992).

$$\hat{\varepsilon} = \frac{\pi^2 S(\hat{c}^2+1)^2}{12(1-v^2)} \tag{15}$$

4. Determine New $\hat{\varepsilon}$ from equation 3.4' of Urbanik (1992).

$$\text{New } \hat{\varepsilon} = \frac{\pi^2 S}{6(1-v^2)}\left(\hat{c} + \sqrt{1-(1-v^2)f(\hat{\varepsilon})}\right) \tag{16}$$

5. If New $\hat{\varepsilon} = \hat{\varepsilon}$, go to Step 7.

6. Otherwise, let $\hat{\varepsilon}$ = New $\hat{\varepsilon}$ and return to Step 4.

7. Retain $\hat{\varepsilon}$ for Step 12 and determine the optimum χ from equation 3.3 of Johnson and Urbanik (1987).

$$\chi = \frac{\pi}{2}\left[1-(1-\nu^2)f(\hat{\varepsilon})\right]^{1/4} \tag{17}$$

Buckling Mode Shape

8. Determine m from Equation (8), integer component m_1 of m, and $m_2 = m_1 + 1$.

9. Determine χ_1 and χ_2 from Equation (9).

10. Set $\chi = \chi_1$ and determine $\hat{\varepsilon}_1$ from Steps 11–15. Then proceed to Step 16.

Finite Length–Fixed χ

11. Input a fixed value of χ.
12. Determine an initial $\hat{\varepsilon}$ from the value retained in Step 7.
13. Determine New $\hat{\varepsilon}$ from equation 3.2' of Urbanik (1992).

$$\text{New}\,\hat{\varepsilon} = \frac{\chi^2 S}{3}\left[\frac{1}{1-\nu^2}\left(\hat{c}+\frac{\pi^2}{4\chi^2}\right)^2 - \frac{\hat{c}^2-1}{1-\nu^2} - f(\hat{\varepsilon})\right] \tag{18}$$

14. If New $\hat{\varepsilon} = \hat{\varepsilon}$, continue.
15. Otherwise, let $\hat{\varepsilon}$ = New $\hat{\varepsilon}$ and return to Step 13.

Buckling Stress

16. Set $\chi = \chi_2$ and repeat Steps 11–15 to determine $\hat{\varepsilon}_2$.
17. Normalized buckling strain $\hat{\varepsilon}$ is lower of $\hat{\varepsilon}_1$ and $\hat{\varepsilon}_2$.
18. Determine normalized buckling stress from equation 5.1 of Johnson and Urbanik (1987).

$$\hat{\sigma} = \tanh\hat{\varepsilon} \tag{19}$$

19. Stop.

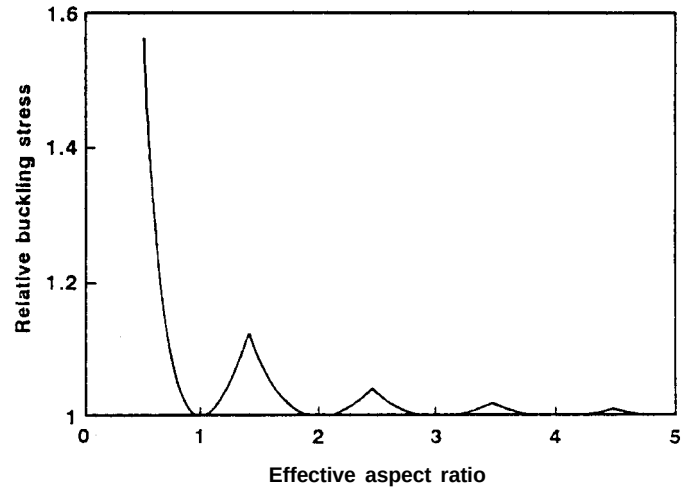

Figure 1. Variation of buckling coefficient K with effective aspect ratio ϕ of plate with linear material. K is buckling stress of a finite length plate with simply supported edges and subjected to axial compression, relative to buckling stress of an infinitely long plate.

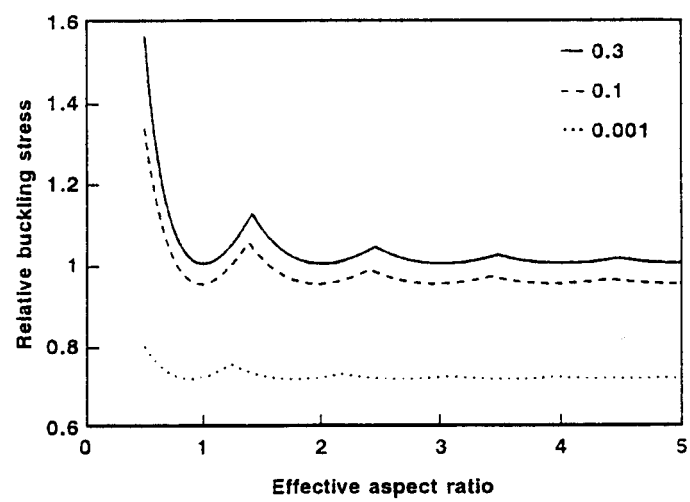

Figure 2. Variation of K with ϕ of plate with nonlinear material. Plots at three levels of normalized plate stiffness S are shown.

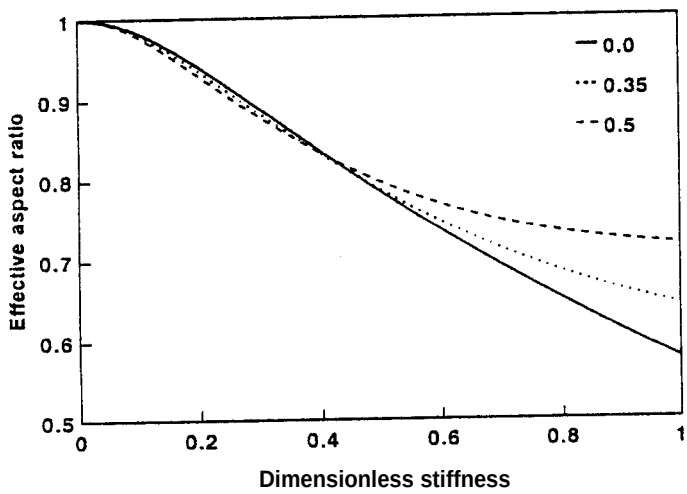

Figure 3. Effective aspect ratio ϕ as a function of normalized stiffness S of plate with nonlinear material, below which plate buckling stress becomes increasingly sensitive to plate length. Variation is plotted for three levels of mean Poisson's ratio *v*.

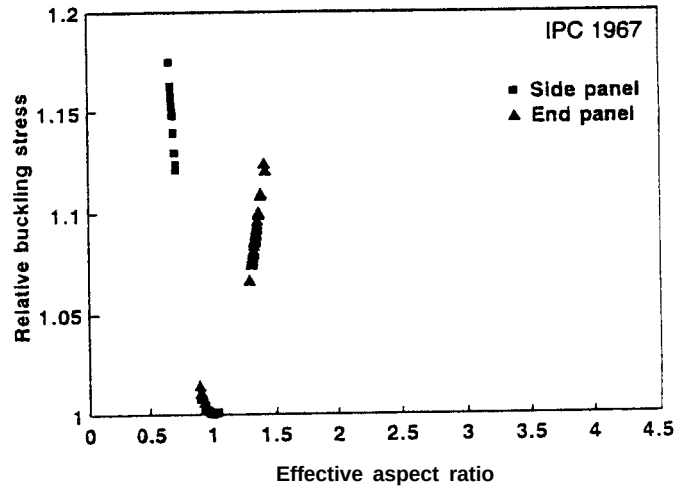

Figure 5. Variation of K with ϕ of corrugated fiberboard box components.

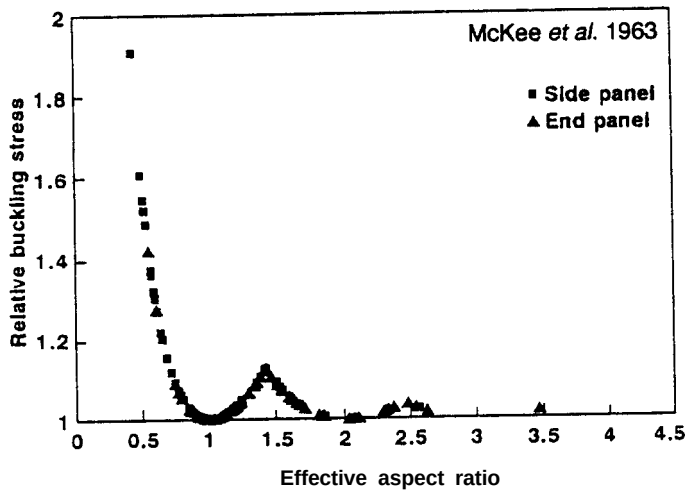

Figure 4. Variation of K with ϕ of corrugated fiberboard box components. Here and in Figs 5-7, material is assumed to have linear behavior.

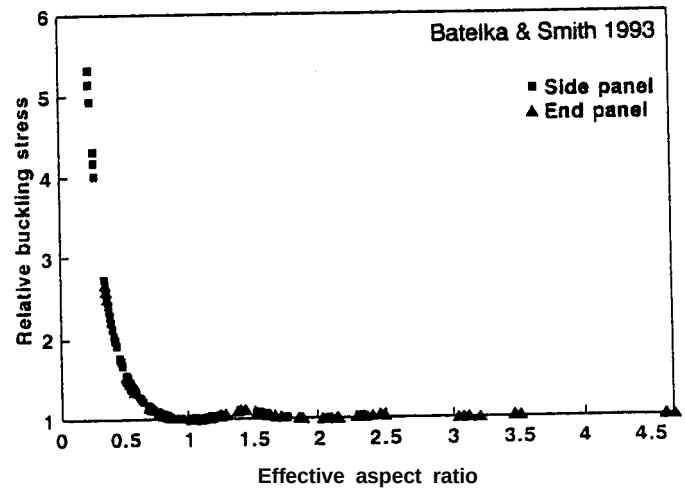

Figure 6. Variation of K with ϕ of corrugated fiberboard tubs components.

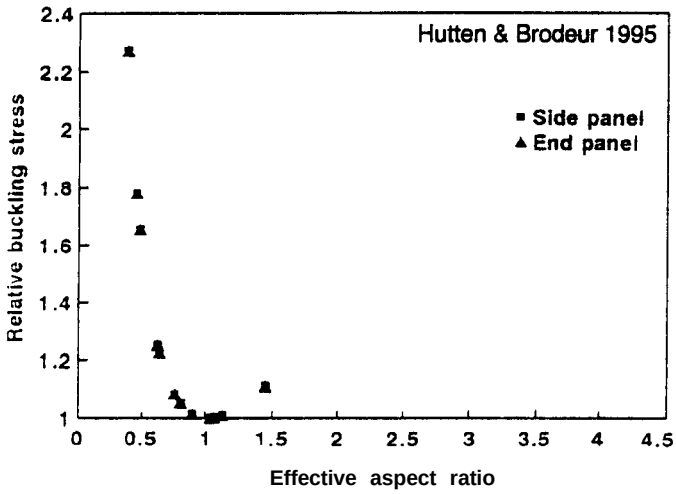

Figure 7. Variation of K with ϕ of corrugated fiberboard tube components.

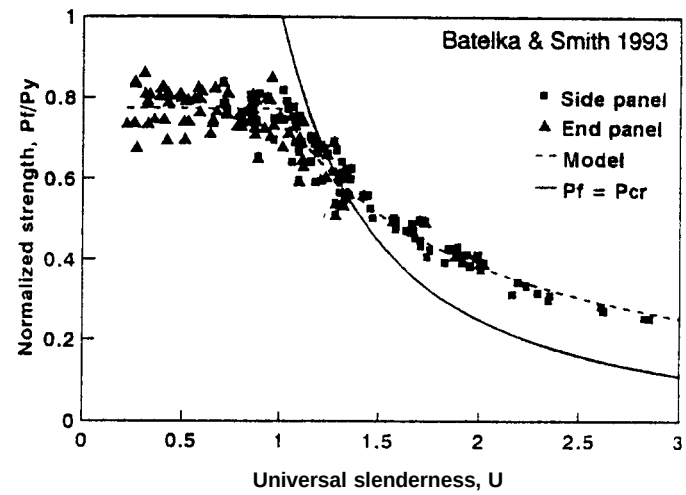

Figure 9. Variation of P_f/P_y with U of supporting panels of corrugated tube. Here and in Figs. 10–13, dashed line is a fit of Eq. (12) to the data, assuming nonlinear material behavior and failure by elastic and inelastic buckling.

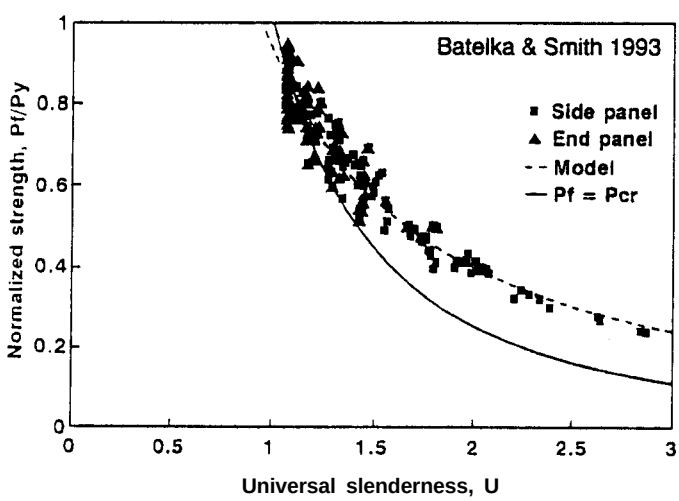

Figure 8. Variation of strength ratio P_f/P_y with universal slenderness U of supporting panels of corrugated tube. Here and in Figs. 9-13, points represent strength of side and end panels scaled as the ratio $2P_f/P$ of experimental strength. Dashed line is a fit of Eq. (11) to the data, assuming nonlinear material behavior and failure by elastic buckling. Here and in Figs. 9–13, solid line corresponds to the condition $P_f = P_{cr}$.

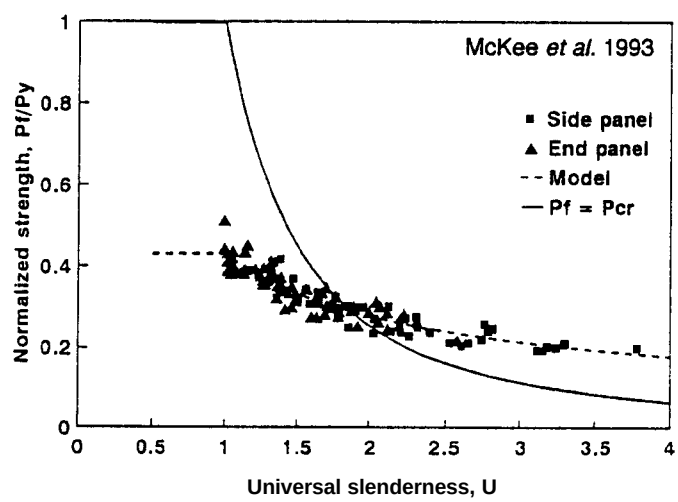

Figure 10. Variation of P_f/P_y with U of supporting panels of corrugated box.

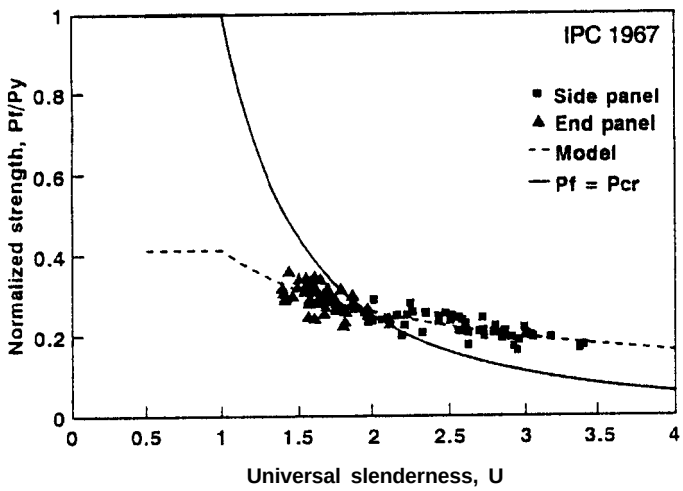

Figure 11. Variation of P_f/P_y with U of supporting panels of

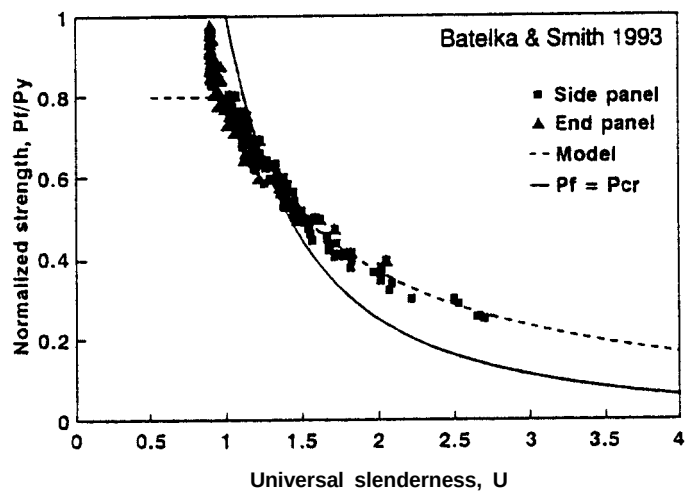

Figure 12. Variation of P_f/P_y with U of supporting panels of corrugated tube.

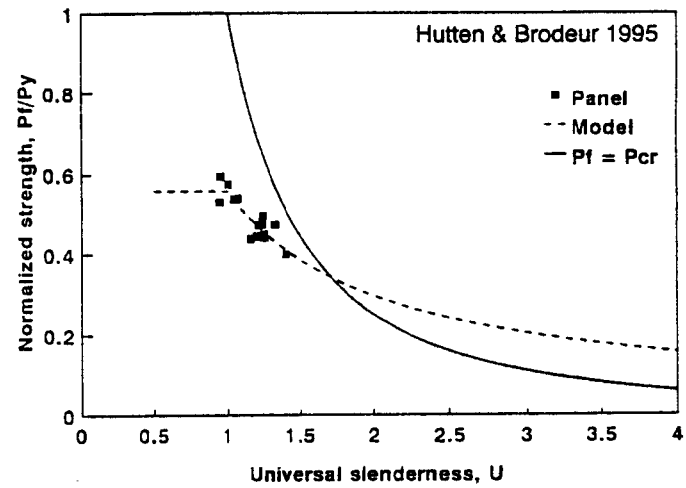

Figure 13. Variation of P_f/P_y with U of supportng panels of corrugated tube.

PVP-Vol. 343

DEVELOPMENT, VALIDATION, AND APPLICATION OF INELASTIC METHODS FOR STRUCTURAL ANALYSIS AND DESIGN

presented at

THE 1996 ASME INTERNATIONAL MECHANICAL ENGINEERING CONGRESS AND EXPOSITION
NOVEMBER 17-22, 1996
ATLANTA, GEORGIA

sponsored by

THE PRESSURE VESSELS AND PIPING DIVISION, ASME

edited by

ROBERT F. SAMMATARO
PROTO-POWER CORPORATION

DOUGLAS J. AMMERMAN
SANDIA NATIONAL LABORATORIES

THE AMERICAN SOCIETY OF MECHANICAL ENGINEERS
United Engineering Center / 345 East 47th Street / New York, N.Y. 10017

Statement from By-Laws: The Society shall not be responsible for statements or opinions advanced in papers. . . or printed in its publications (7.1.3)

Authorization to photocopy material for internal or personal use under circumstance not falling within the fair use provisions of the Copyright Act is granted by ASME to libraries and other users registered with the Copyright Clearance Center (CCC) Transactional Reporting Service provided that the base fee of $4.00 per page is paid directly to the CCC, 27 Congress Street, Salem MA 01970. Requests for special permission or bulk reproduction should be addressed to the ASME Technical Publishing Department.

ISBN No. 0-7918 -1535-8

Library of Congress Number 96-78677

1996 by
THE AMERICAN SOCIETY OF MECHANICAL ENGINEERS
All Rights Reserved
Printed in U.S.A.